

Pionic Atom Spectroscopy in the ($d, {}^3\text{He}$) reaction at finite angles

N. Ikeno, H. Nagahiro, and S. Hirenzaki

Department of Physics, Nara Woman's University, Nara 630-8506, Japan

Received: date / Revised version: date

Abstract. We study the formation of deeply bound pionic atoms in the ($d, {}^3\text{He}$) reactions theoretically and show the energy spectra of the emitted ${}^3\text{He}$ at finite angles, which are expected to be observed experimentally. We find that the different combinations of the pion-bound and neutron-hole states dominate the spectra at different scattering angles because of the matching condition of the reaction. We conclude that the observation of the ($d, {}^3\text{He}$) reaction at finite angles will provide the systematic information of the pionic bound states in each nucleus and will help to develop the study of the pion properties and the partial restoration of chiral symmetry in nuclei.

PACS. 36.10.Gv Mesonic, hyperonic and antiprotonic atoms and molecules – 14.40.Aq pi, K, and eta mesons – 25.45.-z 2H-induced reactions

1 Introduction

Deeply bound pionic atoms were discovered in the ($d, {}^3\text{He}$) spectra in 1996 [1, 2, 3] following the theoretical predictions [4, 5]. They have been considered to be one of the good systems to deduce the pion properties at finite density and to obtain precise information on the partial restoration of chiral symmetry in nuclei [6, 7, 8].

So far, the ($d, {}^3\text{He}$) spectra have been obtained in near recoilless kinematics to observe the peaks of the pionic state formation with a neutron hole in the quasi - substitutional configurations [3, 6, 9]. The Pb and Sn isotopes were used as the target nuclei in the experiments [3, 6, 9] since the spectra were expected to show the peak structures due to one dominant $[\pi \otimes n^{-1}]$ configuration based on the theoretical evaluations [10, 11]. The simple structure of the observed peak is important and effective to deduce the pion binding energies precisely from the observed spectra. Actually, in Ref. [6], the binding energy and width of pionic atoms in Sn isotopes were determined precisely and the partial restoration of chiral symmetry was concluded based on the data.

To develop the studies of pion properties and symmetry restoration in nuclei further, we think that we need to obtain improved information from experiments. Actually, the systematic errors coming from the uncertainties of the neutron distribution and the absolute energy calibration were reported in Ref. [6]. In addition, we need more systematic information on bound states for unique determination of the pion-nucleus interaction, which is required to fix the potential strength related to chiral symmetry. Recently, it was reported in Ref. [12] that the simultaneous observation of various pionic bound states such as $1s$ and $2s$ in the same nucleus may be helpful to reduce

these errors and to develop our studies. Along with this line, in actual experiments, the pionic $2s$ state observation with the $1s$ state has been expected in new high precision experiment in RIBF/RIKEN [12, 13, 14].

In this paper, we consider theoretically the new possibility to observe various pionic bound states in the same nuclei by observing the ($d, {}^3\text{He}$) spectra at finite angles together with the forward direction. These observations at finite angles are expected to be possible in the experiments at RIBF/RIKEN [15]. As well-known in the nuclear inelastic scatterings, we can expect to have the manifestation of different subcomponents of pion and neutron hole states at finite angles due to the matching condition with different momentum transfer, and expect to determine the binding energies and widths of various pionic states simultaneously in each nucleus. The momentum transfer dependence of the effective number was studied in Ref. [5] for different incident energies. The angular dependence of the resonance peak structure will be helpful to determine the angular momentum quantum numbers of the populated states directly from the ($d, {}^3\text{He}$) data.

2 Formulation

We modify slightly the theoretical model used in Refs. [5, 10, 11] to study the angular dependence of the ($d, {}^3\text{He}$) spectra. The modifications are implemented by including the kinematical correction factors K in Eq. (11) as explained below. A similar consideration was also given in Ref. [16] for the (K^-, N) reaction.

We start our discussion by considering the $d + n \rightarrow {}^3\text{He} + \pi^-$ reaction, which is the elementary pion production process for the formation of the pionic atoms in the

($d, {}^3\text{He}$) reaction. Our model is based on the relativistic cross section formula [17] with the Lorentz invariant pion production amplitude $T(p_d, p_n, p_{\text{He}}, p_\pi)$. The cross section can be written as,

$$d\sigma = \frac{1}{v_{\text{rel}}} \frac{M_d}{E_d} \frac{M_n}{E_n} |T(p_d, p_n, p_{\text{He}}, p_\pi)|^2 \times (2\pi)^4 \delta^4(p_d + p_n - p_{\text{He}} - p_\pi) \frac{M_{\text{He}}}{E_{\text{He}}} \frac{d\mathbf{p}_{\text{He}}}{(2\pi)^3} \frac{1}{2E_\pi} \frac{d\mathbf{p}_\pi}{(2\pi)^3}, \quad (1)$$

where the subscript of the momentum p , the energy E and the mass M indicates each particle participating in the two body reaction $d + n \rightarrow {}^3\text{He} + \pi^-$. The relative velocity v_{rel} between d and n can be written as,

$$v_{\text{rel}} = \frac{1}{2E_d E_n} \lambda^{1/2}(s, M_d^2, M_n^2), \quad (2)$$

where s is the Mandelstam variable and λ is the Källén function.

The elementary cross section in the center of mass (CM) frame and the laboratory frame at scattering angle $\theta_{d\text{He}}^{\text{lab}}$, which is required for the effective number approach, are written as

$$\left(\frac{d\sigma}{d\Omega_{\text{He}}}\right)_{\text{ele}}^{\text{CM}} = \frac{|T(p_d, p_n, p_{\text{He}}, p_\pi)|^2 M_d M_n M_{\text{He}}}{(2\pi)^2 \lambda^{1/2}(s, M_d^2, M_n^2)} \times \frac{2|\mathbf{p}_{\text{He}}^{\text{CM}}|^2}{\lambda^{1/2}(s, M_{\text{He}}^2, M_\pi^2)}, \quad (3)$$

and

$$\left(\frac{d\sigma}{d\Omega_{\text{He}}}\right)_{\text{ele}}^{\text{lab}} = \frac{|T(p_d, p_n, p_{\text{He}}, p_\pi)|^2 M_d M_n M_{\text{He}}}{(2\pi)^2 \lambda^{1/2}(s, M_d^2, M_n^2)} \times \left[\frac{|\mathbf{p}_{\text{He}}|^2}{E_\pi |\mathbf{p}_{\text{He}}| + E_{\text{He}} (|\mathbf{p}_{\text{He}}| - |\mathbf{p}_d| \cos \theta_{d\text{He}})} \right]^{\text{lab}}, \quad (4)$$

where the superscripts ‘lab’ and ‘CM’ indicate the frame where the kinematical variables should be evaluated. The ratio of these cross sections can be written as,

$$\left(\frac{d\sigma}{d\Omega_{\text{He}}}\right)_{\text{ele}}^{\text{lab}} / \left(\frac{d\sigma}{d\Omega_{\text{He}}}\right)_{\text{ele}}^{\text{CM}} = \left[\frac{|\mathbf{p}_{\text{He}}|^2}{E_\pi |\mathbf{p}_{\text{He}}| + E_{\text{He}} (|\mathbf{p}_{\text{He}}| - |\mathbf{p}_d| \cos \theta_{d\text{He}})} \right]^{\text{lab}} \times \frac{\lambda^{1/2}(s, M_{\text{He}}^2, M_\pi^2)}{2|\mathbf{p}_{\text{He}}^{\text{CM}}|^2}. \quad (5)$$

This expression can be simplified as,

$$\left(\frac{d\sigma}{d\Omega_{\text{He}}}\right)_{\text{ele}}^{\text{lab}} / \left(\frac{d\sigma}{d\Omega_{\text{He}}}\right)_{\text{ele}}^{\text{CM}} = \frac{|\mathbf{p}_{\text{He}}^{\text{lab}}|^2}{|\mathbf{p}_{\text{He}}^{\text{CM}}|^2}, \quad (6)$$

at forward angles $\theta_{d\text{He}} = 0^\circ$ as shown in Ref. [4,5]. The experimental elementary cross sections in the CM frame were reported in Ref. [18].

Then, we consider the pionic bound state formation cross section for the heavy nuclear target case in the same framework. In the effective number approach used in Refs. [5,10,11], the elementary cross section is factorized from the bound state formation cross section as shown below. The bound state formation cross section for the heavy nuclear target case can be written in the laboratory frame as,

$$d\sigma = \sum_f \frac{V^2}{v_{\text{rel}}} \frac{1}{VT} |S_{fi}|^2 \frac{V}{(2\pi)^3} d\mathbf{p}_{\text{He}}, \quad (7)$$

with the S matrix,

$$S_{fi} = \int dt d\mathbf{x} \sqrt{\frac{M_{\text{He}}}{E_{\text{He}}}} \frac{1}{\sqrt{V}} e^{iE_{\text{He}}t} \chi_{\text{He}}^*(\mathbf{x}) \sqrt{\frac{1}{2E_\pi}} e^{iE_\pi t} \phi_\pi^*(\mathbf{x}) \times iT(p_d, p_n, p_{\text{He}}, p_\pi) \times \sqrt{\frac{M_d}{E_d}} \frac{1}{\sqrt{V}} e^{-iE_d t} \chi_d(\mathbf{x}) \sqrt{\frac{M_n}{E_n}} e^{-iE_n t} \psi_n(\mathbf{x}), \quad (8)$$

where ϕ_π and ψ_n indicate the wavefunctions of the pion bound state in the daughter nucleus and the neutron bound state in the target nucleus, respectively. The wavefunctions of the projectile (d) and the ejectile (${}^3\text{He}$) are denoted by χ_{He}^* and χ_d . $T(p_d, p_n, p_{\text{He}}, p_\pi)$ indicates the same meson production amplitude appeared in Eq. (1) and describe the $d + n \rightarrow {}^3\text{He} + \pi^-$ transition. V and T indicate the spatial volume and the time interval for the transition [17]. We assume that only the neutron in the target nucleus participates in the reaction and other nucleons are spectators. The formation cross section of the pion bound states in the laboratory frame can be expressed as,

$$\left(\frac{d^2\sigma}{dE_{\text{He}} d\Omega_{\text{He}}}\right)_A^{\text{lab}} = \sum_f \left[\frac{1}{2(2\pi)^2} \frac{M_d M_n M_{\text{He}}}{E_n E_\pi} \frac{|\mathbf{p}_{\text{He}}|}{|\mathbf{p}_d|} \times |T(p_d, p_n, p_{\text{He}}, p_\pi)|^2 \frac{\Gamma}{2\pi} \frac{1}{\Delta E^2 + \Gamma^2/4} \times \left| \int d\mathbf{x} \chi_{\text{He}}^*(\mathbf{x}) \phi_\pi^*(\mathbf{x}) \psi_n(\mathbf{x}) \chi_d(\mathbf{x}) \right|_A^2 \right]^{\text{lab}}, \quad (9)$$

where the subscript ‘A’ indicates the ($d, {}^3\text{He}$) reaction for the nuclear target. Here, we assume that the target nucleus is so heavy that we can ignore the recoil energy of the nucleus and that we can consider the CM and the laboratory frames to be the same. The δ -function responsible for the energy conservation is replaced by the Lorentz distribution function $\frac{\Gamma}{2\pi} \frac{1}{\Delta E^2 + \Gamma^2/4}$ to account for the width Γ of the pion bound state, where ΔE is defined as $\Delta E = E_{\text{He}} + E_\pi - E_d - E_n$. E_n is the energy of neutron in the target nucleus and defined as $E_n = M_n - S_n(j_n)$ with the neutron separation energy S_n from the j_n single particle level and the neutron mass M_n . E_π is the energy of the pion bound state defined as $E_\pi = M_\pi - B.E.(\ell_\pi)$ with the pion mass M_π and the binding energy $B.E.$ of the bound state indicated by ℓ_π . The reaction Q -value can be expressed as

$Q = \Delta E - M_\pi + B.E.(\ell_\pi) - S_n(j_n) + (M_n + M_d - M_{\text{He}})$, where $M_n + M_d - M_{\text{He}} = 6.787$ MeV.

We express the effective number for each eigen state of the total spin of neutron-hole and pion-particle states in the daughter nuclei. We decompose the sum of the final states as

$$\sum_f \rightarrow \sum_{ph} \sum_{JM}, \quad (10)$$

where \sum_{ph} indicates the sum of all combinations of the pion bound states and neutron hole states in the final states, and \sum_{JM} indicates the sum of the states with different total angular momentum for each combination of bound pion and neutron hole state. By neglecting the residual interaction effects for the final state energies, we can rewrite the bound state formation cross section as,

$$\left(\frac{d^2\sigma}{dE_{\text{He}}d\Omega_{\text{He}}} \right)_A^{\text{lab}} = \left(\frac{d\sigma}{d\Omega_{\text{He}}} \right)_{\text{ele}}^{\text{lab}} \times \sum_{ph} K \frac{\Gamma}{2\pi} \frac{1}{\Delta E^2 + \Gamma^2/4} N_{\text{eff}}, \quad (11)$$

where we have used the elementary cross section $\left(\frac{d\sigma}{d\Omega_{\text{He}}} \right)_{\text{ele}}^{\text{lab}}$ instead of $|T|^2$. The effective number N_{eff} defined as,

$$N_{\text{eff}} = \sum_{JM} \left| \int d\mathbf{r} \chi_{\text{He}}^*(\mathbf{r}) [\phi_{\ell_\pi}^*(\mathbf{r}) \otimes \psi_{j_n}(\mathbf{r})]_{JM} \chi_d(\mathbf{r}) \right|^2. \quad (12)$$

We introduce the distortion effects to the wavefunctions χ_{He}^* and χ_d by Eikonal approximation as described in Refs. [5, 10, 11]. The kinematical correction factor K is derived by factorizing the elementary cross section in the laboratory frame Eq. (4) from the bound state formation cross section for the heavy nuclear target case Eq. (9), and is defined as,

$$K = \left[\frac{|\mathbf{p}_{\text{He}}^A|}{|\mathbf{p}_{\text{He}}|} \frac{E_n E_\pi}{E_n^A E_\pi^A} \left(1 + \frac{E_{\text{He}}}{E_\pi} \frac{|\mathbf{p}_{\text{He}}| - |\mathbf{p}_d| \cos\theta_{d\text{He}}}{|\mathbf{p}_{\text{He}}|} \right) \right]^{\text{lab}}, \quad (13)$$

where A indicates the momentum and energy which should be evaluated in the kinematics of the nuclear target case. Since we consider the heavy target limit, the scattering angle of nuclear target case does not appear in Eq. (13). It should be noted that in addition to the wavefunctions ϕ_{ℓ_π} and ψ_{j_n} , ΔE , Γ and K also depend on the final ‘ ph ’ combination through the binding energy and width of the pion bound states and neutron separation energy. The K factor is evaluated by the energy and momentum at the kinematics satisfying the condition $\Delta E = 0$ for each ‘ ph ’ combination. This correction factor is $K = 1$ for the recoilless kinematics at $\theta_{d\text{He}}^{\text{lab}} = 0^\circ$ with $S_n = 0$ and $B.E. = 0$.

Here, we have assumed the same meson production amplitude $T(p_d, p_n, p_{\text{He}}, p_\pi)$ for the pion bound state formation process in the heavy nucleus as the elementary

Table 1. Elementary cross sections in CM frame $(d\sigma/d\Omega)_{\text{ele}}^{\text{CM}}$ and those in lab frame $(d\sigma/d\Omega)_{\text{ele}}^{\text{lab}}$ in unit of $[\mu\text{b}/\text{sr}]$. The scattering angles $\theta_{d\text{He}}^{\text{lab}}$ and $\theta_{d\text{He}}^{\text{CM}}$ indicate the angles between deuteron and ${}^3\text{He}$ in the $d + n \rightarrow {}^3\text{He} + \pi^-$ reactions in CM and lab frames, respectively. We use Eq. (14) to fit the experimental data in Ref. [18].

$\theta_{d\text{He}}^{\text{lab}}$	0.0°	1.0°	2.0°	3.0°
$\left(\frac{d\sigma}{d\Omega} \right)_{\text{ele}}^{\text{lab}}$	1.77×10^3	1.70×10^3	1.50×10^3	1.22×10^3
$\theta_{d\text{He}}^{\text{CM}}$	0.0°	15.0°	31.0°	49.5°
$\left(\frac{d\sigma}{d\Omega} \right)_{\text{ele}}^{\text{CM}}$	8.00	7.48	6.05	4.02

process by the impulse approximation. We need to know the microscopic mechanisms of the meson production to evaluate the possible modifications of the T amplitude beyond the kinematical corrections.

As a summary of this section, we use Eq. (11) to calculate the angular dependence of the pionic atom formation spectra. This formula newly include the kinematical correction factor K which has a certain contribution to the angular dependence of the cross section as we will see later. As for the elementary cross section, we obtain $\left(\frac{d\sigma}{d\Omega_{\text{He}}} \right)_{\text{ele}}^{\text{lab}}$ in Eq. (11) by the formula Eq. (5) from the cross section in the CM frame which have been determined experimentally [18].

3 Numerical Results and Discussions

First, we consider the angular dependence of the elementary cross section. As the elementary cross section, we have used the experimental data of $p + d \rightarrow t + \pi^+$ reaction reported in Ref [18] in the CM frame by isospin symmetry. We parameterize the data shown in Fig. 5 in Ref [18] as,

$$\left(\frac{d\sigma}{d\Omega} \right)_{\text{ele}}^{\text{CM}} = 10^{-0.852 \cos(\pi - \theta_{d\text{He}}^{\text{CM}}) + 0.051} [\mu\text{b}/\text{sr}], \quad (14)$$

and transfer the cross section to that in the lab frame by Eq. (5). We show the values of elementary cross sections used in this paper in Table 1.

We, then, show the differences of the kinematics between the elementary process $d + n \rightarrow {}^3\text{He} + \pi^-$ and the meson bound state production $A(d, {}^3\text{He})(A-1) \otimes \pi^-$ with a heavy nucleus target. We show in Fig. 1 the momentum transfer \mathbf{q} at $\theta_{d\text{He}}^{\text{lab}} = 0^\circ$ and 2° for the elementary process and the reaction with the heavy nuclear target for pion production with the meson binding energy $B.E. = 0$ and the neutron separation energy $S_n = 0$. We find that the recoilless condition ($|\mathbf{q}| = 0$) is only satisfied at $\theta_{d\text{He}}^{\text{lab}} = 0^\circ$ at $T_d = 455$ MeV for both reactions. At different incident energy, the momentum transfer takes obviously different

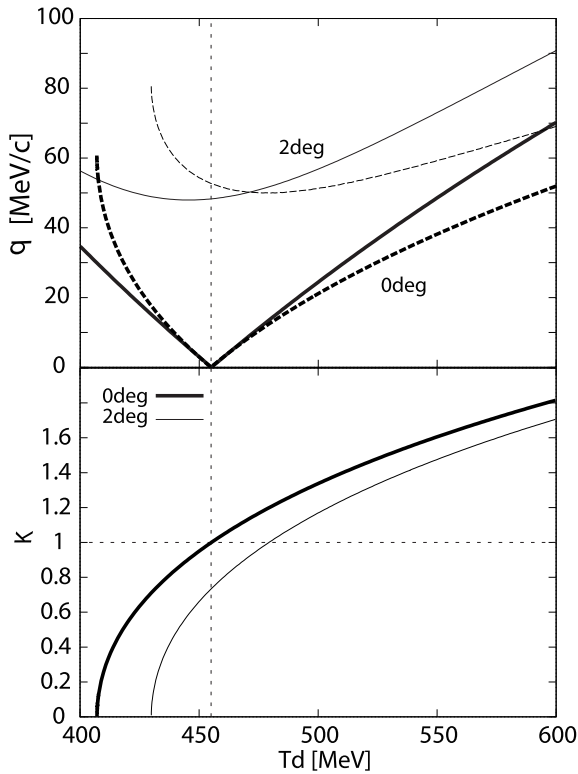


Fig. 1. Momentum transfer q (upper) and kinematical correction factors K (lower) of the $(d, {}^3\text{He})$ reaction at $\theta_{d\text{He}}^{\text{lab}} = 0^\circ$ (thick lines) and 2° (thin lines) plotted as functions of the incident deuteron kinetic energy T_d . In the upper frame, the solid lines show the results for the formation of π meson in the heavy target nucleus, and the dashed lines those for the elementary process. The pion binding energy $B.E.$ and the neutron separation energy S_n from the target nucleus are assumed to be 0 MeV. The vertical line indicates the incident energy T_d satisfying the recoilless condition at $\theta_{d\text{He}}^{\text{lab}} = 0^\circ$.

value for these two reactions. We also show the incident deuteron energy dependence of the K factor in Fig. 1. We found that the K factor is 1 for the recoilless kinematics with $B.E. = 0$ and $S_n = 0$ as naturally expected. The K factor is 0 at $T_d = 407$ MeV and $T_d = 430$ MeV for $\theta_{d\text{He}}^{\text{lab}} = 0^\circ$ and 2° , respectively. These energies correspond to the pion production threshold for the elementary process. And the K factor increases with the incident deuteron kinetic energy T_d .

In Fig. 2, we show the momentum transfer for the nuclear target case and the K factor for $T_d = 500$ MeV at $\theta_{d\text{He}}^{\text{lab}} = 0^\circ$ and 2° as functions of the reaction Q -value, which is the kinematics considered in the missing mass spectroscopy of the deeply bound pionic atoms in this article. We find that the K factor gradually varies about 10% within the Q -value range considered here for both $\theta_{d\text{He}}^{\text{lab}} = 0^\circ$ and 2° cases, and the K factor decreases about 20% at $\theta_{d\text{He}}^{\text{lab}} = 2^\circ$ from the value at $\theta_{d\text{He}}^{\text{lab}} = 0^\circ$. Thus, we think the K factor should be introduced to study the angular dependence of the $(d, {}^3\text{He})$ spectra.

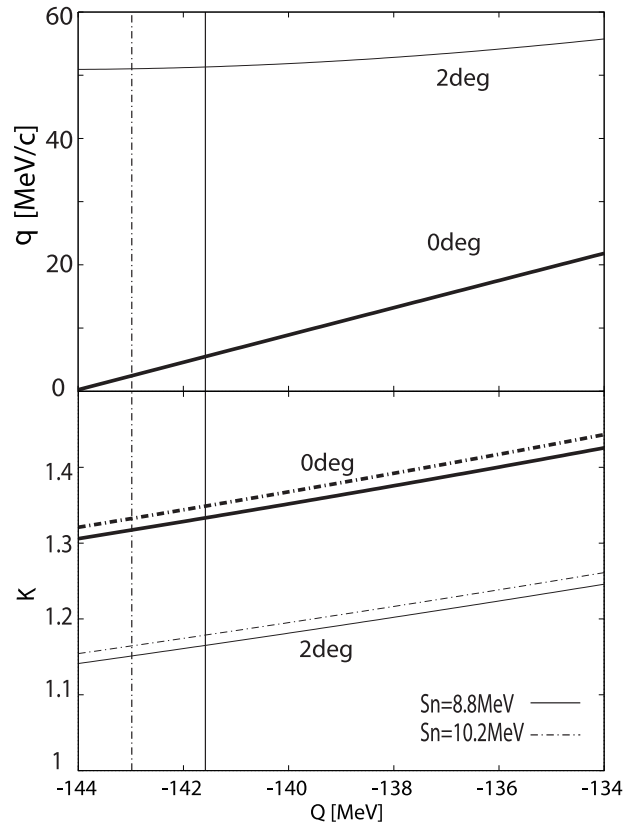


Fig. 2. Momentum transfer q (upper) and kinematical correction factors K (lower) of the $(d, {}^3\text{He})$ reaction at $\theta_{d\text{He}}^{\text{lab}} = 0^\circ$ and 2° for the formation of π meson bound states in the heavy target nucleus plotted as functions of the reaction Q -value. The incident deuteron kinetic energy is fixed to be $T_d = 500$ MeV. The neutron separation energy S_n is fixed to be 8.8 MeV (solid lines) and 10.2 MeV (dash-dotted lines). The vertical lines indicate the π meson production threshold for $S_n = 8.8$ and 10.2 MeV cases.

In Fig. 3, we show the calculated $(d, {}^3\text{He})$ spectra at finite angles for the bound pionic states formation. Two kinds of the neutron wavefunction have been used for the calculations, which are the harmonic oscillator wavefunction and the calculated wavefunction using the neutron potential reported in Ref. [19]. Though the absolute value of the calculated cross sections depend on the neutron wavefunction used as shown in Ref. [12], the angular dependence of the spectra resembles each other. We find that the spectra have a strong angular dependence and the shape of the spectra are much different at finite angles from that at 0° . The largest peak structure at $Q = -137.8$ MeV in the forward spectra is strongly suppressed at finite angles and the spectra show the structure of three peaks at $\theta_{d\text{He}}^{\text{lab}} \geq 2^\circ$. The overall strength of the spectra has also angular dependence and is smaller for larger angles.

In Fig. 4, we show the dominant subcomponents of $(d, {}^3\text{He})$ spectra for each scattering angle $\theta_{d\text{He}}^{\text{lab}}$. Here, we have used the neutron wavefunction obtained by the potential in Ref. [19] and we have also shown the spectra with better energy resolution 100 keV case. At $\theta_{d\text{He}}^{\text{lab}} =$

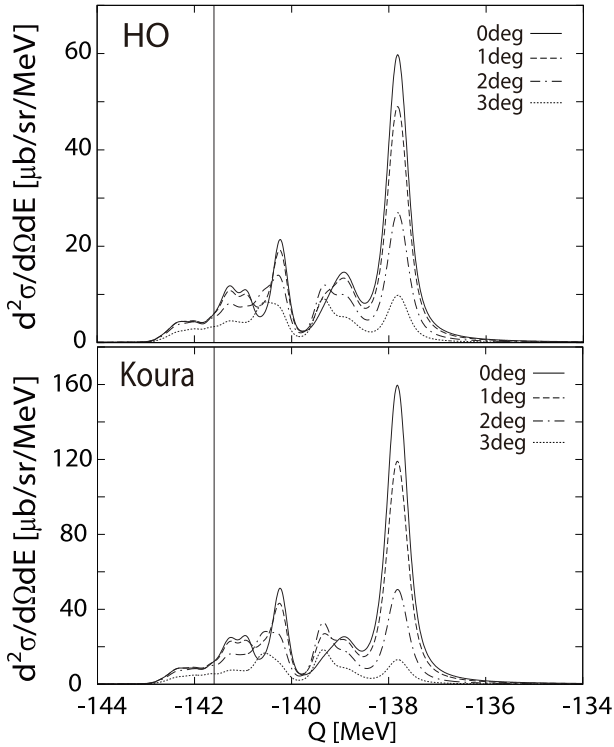


Fig. 3. Calculated ${}^{122}\text{Sn}(d, {}^3\text{He})$ spectra for the formation of the pionic bound states at $\theta_{d\text{He}}^{\text{lab}} = 0^\circ$ (solid lines), 1° (dash lines), 2° (dash-dotted lines) and 3° (dotted lines) plotted as functions of the reaction Q -value. The harmonic oscillator (upper) and the phenomenological [19] (lower) neutron wavefunctions are used. The incident deuteron kinetic energy is fixed to be $T_d = 500$ MeV. The instrumental energy resolution is assumed to be 300 keV FWHM. The vertical line indicates the pion production threshold $Q = -141.6$ MeV.

0° , since the reaction is close to recoilless, the peaks of $[(1s)_\pi \otimes (3s_{1/2})_n^{-1}]$ and $[(2s)_\pi \otimes (3s_{1/2})_n^{-1}]$ subcomponents appear clearly in the spectra for both energy resolution cases. The contributions of $(3s)_\pi$ and $(4s)_\pi$ also show the isolated peaks for better energy resolution (100 keV) case even though they are small. At $\theta_{d\text{He}}^{\text{lab}} = 1^\circ$, the contribution for $[(2s)_\pi \otimes (3s_{1/2})_n^{-1}]$ is suppressed and can only be seen clearly in a better energy resolution case. At larger angles, the pionic $(2p)$ state contributions become relatively larger and dominate the peak structure around $Q = -139.4$ MeV and -140.4 MeV. We can expect to observe the peak structure composed from $[(2p)_\pi \otimes (3s_{1/2})_n^{-1}]$, $[(2p)_\pi \otimes (2d_{3/2})_n^{-1}]$ and $[(2p)_\pi \otimes (1h_{11/2})_n^{-1}]$ subcomponents. Though, the separation energies of these 3 neutron levels differ from each other only within 60 keV [12] and their contributions can not be distinguished, we can expect to deduce the information on the pionic $2p$ state. These contributions of pionic $2p$ state can not be seen in the spectra at $\theta_{d\text{He}}^{\text{lab}} = 0^\circ$ since they are hidden in the tail of the large $1s$ contributions. At finite angles, due to the significant suppression of the $1s$ contributions, the $2p$ contributions can be observed even if they are a little smaller

than those at the forward angle. Thus, to observe the spectra at finite angle is valuable.

Finally, we comment on the small peak structures in the pionic unbound energy region which appear in better energy resolution cases in Fig. 4 right panels. They are the contributions of lightly bound pionic atom formation with one of the deep neutron hole states corresponding to the excited states of the daughter nucleus such as $[(3p)_\pi \otimes (2d_{5/2})_n^{-1}]$, $[(4p)_\pi \otimes (2d_{5/2})_n^{-1}]$, $[(3d)_\pi \otimes (2d_{5/2})_n^{-1}]$, $[(4d)_\pi \otimes (2d_{5/2})_n^{-1}]$ and so on. The wavefunctions of the lightly bound pionic atom have large spatial dimensions and small overlaps with nucleon wavefunction, and thus, both widths and formation cross sections of these bound states are small. Therefore, we can observe contributions of these states formations only in the spectra with better energy resolution.

4 Summary

We study the formation of deeply bound pionic atoms in the ($d, {}^3\text{He}$) reactions theoretically and show the angular dependence of the expected spectra, which can be observed in experiments.

We develop the formula to include the kinematical correction factors to the effective number approach to obtain more realistic angular dependence of the ($d, {}^3\text{He}$) spectra. We show the behavior of the kinematical correction factor and the angular dependence of the ${}^{122}\text{Sn}(d, {}^3\text{He})$ spectra at $T_d = 500$ MeV for the formation of the pionic atoms.

We find that the spectra are dominated by the subcomponents including $(2p)_\pi$ state at larger scattering angles $\theta_{d\text{He}}^{\text{lab}} \geq 2^\circ$, while they are dominated by the $(1s)_\pi$ and $(2s)_\pi$ states at forward angles. The peaks are well isolated and can be observed in the experiments with the good energy resolution. Thus, we can conclude that we can obtain information of deeply bound pionic $2p$ state in addition to $1s$ and $2s$ states by observing the spectra at finite angles. As indicated in Ref. [12], the observation of several deeply pionic bound states in a certain nucleus will help to deduce precise information of pion properties and the chiral dynamics at finite density [6, 7, 8]. We believe that our results provide a good evaluation for further experimental studies of the states reported here, which should contribute to the development of the field.

Acknowledgments

We acknowledge the fruitful discussions with K. Itahashi, S. Itoh, T. Nishi and D. Jido. N. I. appreciates the support by the Grant-in-Aid for JSPS Fellows (No. 23-2274). This work was partly supported by the Grants-in-Aid for Scientific Research (No. 20540273 and No. 22105510).

References

1. T. Yamazaki *et al.*, *Z. Phys.* **A355**, (1996) 219.

2. H. Gilg *et al.*, Phys. Rev. **C62**, (2000) 025201.
3. K. Itahashi *et al.*, Phys. Rev. **C62**, (2000) 025202.
4. H. Toki, S. Hirenzaki, T. Yamazaki and R. S. Hayano, Nucl. Phys. **A501**, (1989) 653.
5. S. Hirenzaki, H. Toki and T. Yamazaki, Phys. Rev. **C44**, (1991) 2472;
H. Toki, S. Hirenzaki and T. Yamazaki, Nucl. Phys. **A530**, (1991) 679.
6. K. Suzuki *et al.*, Phys. Rev. Lett. **92**, (2004) 072302.
7. E. E. Kolomeitsev, N. Kaiser and W. Weise, Phys. Rev. Lett. **90**, (2003) 092501.
8. D. Jido, T. Hatsuda and T. Kunihiro, Phys. Lett. **B670**, (2008) 109.
9. H. Geissel *et al.*, Phys. Lett. **B549**, (2002) 64.
10. Y. Umemoto, S. Hirenzaki, K. Kume and H. Toki, Phys. Rev. **C62**, (2000) 024606.
11. Y. Umemoto, S. Hirenzaki, K. Kume and H. Toki, Prog. Theor. Phys. **103**, (2000) 337.
12. N. Ikeno, R. Kimura, J. Yamagata-Sekihara, H. Nagahiro, D. Jido, K. Itahashi, L. S. Geng and S. Hirenzaki, Prog. Theor. Phys. **126**, (2011) 483.
13. K. Itahashi *et al.*, 'Precision Spectroscopy of Pionic Atoms in ($d, {}^3\text{He}$) Nuclear Reactions'; Exp. proposal NP0702-RIBF-027 for RIBF, Dec. (2006).
14. K. Itahashi *et al.*, 'Spectroscopy of Pionic Atom in ${}^{122}\text{Sn}(d, {}^3\text{He})$ Nuclear Reaction'; Exp. proposal NP0802-RIBF-054 for RIBF, Jan. (2008).
15. S. Itoh, 'Precision Spectroscopy of Pionic Atom at RIKEN-RIBF', Talk given at XIV International Conference on Hadron Spectroscopy (Hadron 2011) 13 - 17 June 2011, München, Germany;
K. Itahashi, private communication.
16. T. Koike and T. Harada, Nucl. Phys. **A804**, (2008) 231.
17. For example, J. D. Bjorken and S. D. Drell, Relativistic Quantum Mechanics, McGraw-Hill Book Company, 1964.
18. M. Betigeri *et al.*, Nucl. Phys. **A690**, (2001) 473.
19. H. Koura and M. Yamada, Nucl. Phys. **A671**, (2000) 96.

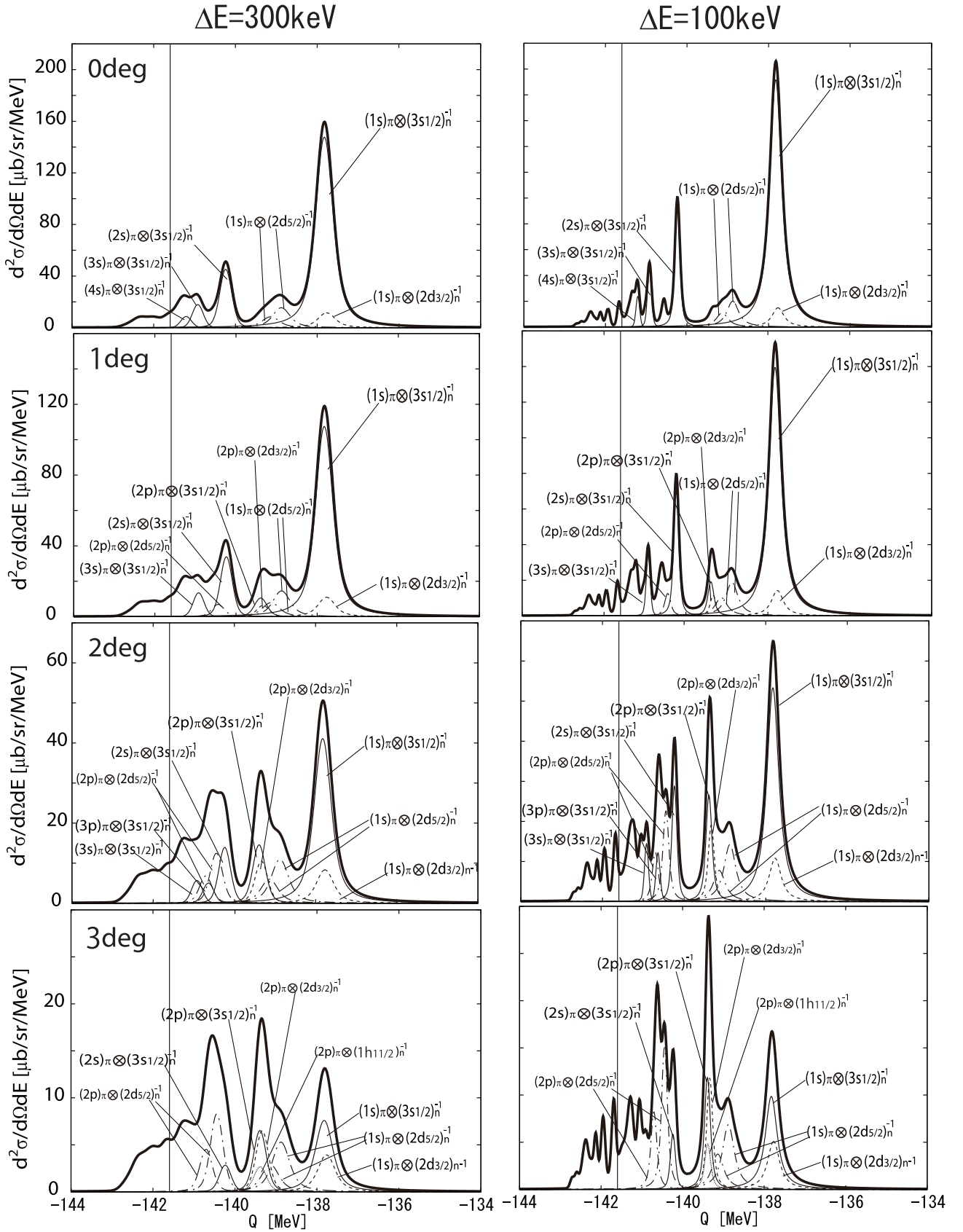


Fig. 4. Calculated ${}^{122}\text{Sn}(d, {}^3\text{He})$ spectra for the formation of the pionic bound states at $\theta_{d\text{He}}^{\text{lab}} = 0^\circ, 1^\circ, 2^\circ$ and 3° are plotted as functions of the reaction Q -value. Dominant subcomponents $[(nl)\pi \otimes (nl_j)_n^{-1}]$ are indicated in the figure. The phenomenological neutron wavefunctions [19] are used. The instrumental energy resolution is assumed to be 300 keV FWHM (left) and 100 keV FWHM (right). The vertical line indicates the pion production threshold $Q = -141.6$ MeV.